Carbohydrate Polymers 87 (2012) 839–845

Contents lists available at SciVerse ScienceDirect

Carbohydrate Polymers

journal homepage: www.elsevier.com/locate/carbpol

Antimicrobial activity of silver nanoparticle impregnated bacterial cellulose membrane: Effect of fermentation carbon sources of bacterial cellulose

Guang Yang[a,*], Jianjian Xie[a], Feng Hong[a,b], Zhangjun Cao[a], Xuexia Yang[a]

[a] Group of Microbiological Engineering and Industrial Biotechnology, College of Chemistry, Chemical Engineering and Biotechnology, Donghua University, Shanghai, 201620, China
[b] State Key Laboratory for Modification of Chemical Fibers and Polymer Materials, Donghua University, Shanghai 201620, China

ARTICLE INFO

Article history:
Received 26 July 2011
Received in revised form 16 August 2011
Accepted 23 August 2011
Available online 31 August 2011

Keywords:
Bacterial cellulose
Silver nanoparticle
Template synthesis
Antimicrobial activity
Fermentation carbon sources

ABSTRACT

Bacterial cellulose (BC), a natural nanoporous matrix, was utilized as the template to in situ synthesize silver nanoparticles (AgNPs) by chemical reduction. Effects of the microstructure of the BC template, produced by different fermentation carbon sources were investigated on the formation of AgNPs. A detailed characterization, e.g. SEM, XRD and nitrogen physisorption for pure BC, and EDX, UV–vis spectroscopy, TEM and inductively coupled plasma for the AgNPs impregnated BC composites (BC/AgNPs) were done, and the antimicrobial activity of every composite was evaluated by both zone of inhibition and log reduction methods. It was revealed that the particle size of AgNPs, and the silver content and antimicrobial activity of the BC/AgNPs composites varied depending on the different BC templates used, mainly due to the differences in the microstructure of the BC template, especially the crystallinity and porous properties. As far as we know, little studies have been done on this issue.

1. Introduction

The development of modern wound dressing based on novel biomaterials has attracted more and more attentions in the past few years, varying from alginates (Wiegand, Heinze, & Hipler, 2009) to chitosan (Clasen, Wilhelms, & Kulicke, 2006) and hyaluronic acid (Uppal, Ramaswamy, Arnold, Goodband, & Wang, 2011). In recent years, bacterial cellulose (BC), a polymer synthesized by the acetic acid bacterium *Gluconacetobacter xylinus* (formerly *Acetobacter aceti* subsp. *xylinus* or *A. xylinus*), is being received as a natural power to heal wounds (Czaja, Krystynowicz, Bielecki, & Brown, 2006). While chemically the same as plant cellulose, bacterial cellulose features a distinctive 3-D structure consisting of an ultrafine network of cellulose nanofibers (Czaja, Young, Kawecki, & Brown, 2007). This unique micromorphology determines its distinguished physical and mechanical properties, e.g. high porosity, excellent mechanical strength and large surface area (Jonas & Farah, 1998), which can supply as an excellent wound healing system with high water holding ability, great sorption of liquids, good conformability and excellent wet strength. However, bacterial cellulose itself has no antimicrobial activity and cannot provide a barrier against wound infection, which is a major factor common to all wound care, especially the burn wounds, traumatic injuries and surgical procedures (Robson, 1997). To resolve this, many efforts were made to associate antibacterial agents with the bacterial cellulose membrane for the sake of developing new biomedical materials with antimicrobial activity (Hu et al., 2009; Maneerung, Tokura, & Rujiravanit, 2008; Wei, Yang, & Hong, 2011).

Silver is known to be a broad-spectrum agent effective against a large number of Gram-positive and Gram-negative microorganisms, many aerobes and anaerobes, and several antibiotic resistant strains (Klasen, 2000a, 2000b); therefore there is a strong incentive to develop silver-contained drugs and dressings to comprise a pattern of antimicrobial topical treatments for wound care (Lansdown, 2002; Leaper, 2006). In the present century, silver nanoparticles (AgNPs) have come up as one of the most effective antibacterial agents due to their large surface area to volume ratio comparable to the bulk form (Rai, Yadav, & Gade, 2009). However, at the nanometric level, a crucial issue about AgNPs is their tendency to aggregate, thus losing the peculiar properties related with the nanoscale. One strategy to prevent aggregation is the controlled deposition of metal particles through hybridization with a nanoporous material as the template to ensure a well-defined spatial distribution (Cai, Kimura, Wada, & Kuga, 2009; Lee, Mao, Flynn, & Belcher, 2002). The reported examples of templates included polymers (Bhattacharjee & Mandal, 2007; Cui, Liu, Li, Zhou, & Xu, 2010), surfactants (Wu, Kuga, & Huang, 2008), DNA (Nyamjav & Ivanisevic, 2005) and so on.

In recent years, bacterial cellulose, which possesses high open porosity, near transparency, large surface area and high mechanical

* Corresponding author at: College of Chemistry, Chemical Engineering and Biotechnology, Donghua University, North Ren Min Road, No. 2999, Songjiang, Shanghai, 201620, China. Tel.: +86 21 67792749; fax: +86 21 67792649.
E-mail address: gyang@dhu.edu.cn (G. Yang).

0144-8617/$ – see front matter © 2011 Elsevier Ltd. All rights reserved.
doi:10.1016/j.carbpol.2011.08.079

strength, have been recommended to be the template matrix for metal nanoparticle synthesis (Li et al., 2009). Some researchers have studied in situ synthesis of AgNPs on BC membrane by immersing it into silver precursor, $AgNO_3$ solution, and then in situ reduction with $NaBH_4$ as the reducing agent (Maneerung et al., 2008). It was pointed out that during the synthesis process, the BC membrane first coordinated Ag ions (Ag^+) to form a BC-Ag^+ complex; then the absorbed silver ion inside the BC matrix was reduced to the metallic silver nanoparticles (Ag^0). The nanosized pores of the BC material were acted as the nanoreactors for the nucleation and growth of the nanoparticles, and they could also restrict the growth of particles within the pores, resulting in a small size and a narrow size distribution (Barud et al., 2008; Cai et al., 2009; Hu et al., 2009; Maneerung et al., 2008). In that case, it could be speculated that the nano-structure of the BC membrane played a crucial role in the formation of Ag nanoparticles as well as their structure characteristics including the size and size distribution, and the loading amount, which directly determined the antimicrobial properties of the AgNPs impregnated BC composite (BC/AgNPs composite).

In our previous work, we have found that the micro-structures of the BC membrane, e.g. the surface area, pore volume and crystallinity could be altered by changing the fermentation medium especially carbon sources under the static culture conditions. Hence, in this study, we wish to further prepare the AgNPs impregnated BC composite by template synthesis. Specially, the influences of the micro-structure of the template matrix, i.e. the BC membrane herein, were investigated on the in situ synthesis of the silver nanoparticles. A detailed characterization of these BC/AgNPs composites was done, and their antimicrobial activities were determined by using *Escherichia coli* (Gram negative) and *Staphylococcus aureus* (Gram positive) as the model bacteria. As far as we know, little studies have been done on this issue. We anticipate that this study might have a beneficial support for future biomedical application of bacterial cellulose with antimicrobial properties.

2. Materials and methods

2.1. Bacterial strain and culture medium

G. xylinus (formerly *Acetobacter aceti* subsp. *xylinus* or *A. xylinus*) (strain 1.1812), *E. coli* (strain 1.1100) and *S. aureus* (strain1.128) were purchased from Institute of Microbiology Chinese Academy of Science and maintained on solid agar medium at 4 °C. Both the seed medium and fermentation medium used for BC production contained 2.5 (w/v%) carbon source, 0.3 (w/v%) tryptone and 0.5 (w/v%) yeast extract. The carbon sources investigated here included glucose, maltose and sucrose. Prior to sterilization at 121 °C, the pH value of the medium was adjusted to 5.0.

2.2. Preparation of BC membrane

Pre-inoculum for all experiments was conducted by transferring a single *G. xylinus* colony grown on agar culture medium into a 250-ml Erlenmeyer flask filled with 100 ml of seed culture medium. After agitated cultivation of 24 h at 30 °C, 6 ml of the cell suspension was introduced into a 250-ml Erlenmeyer flask containing 100 ml of fermentation culture medium, and then incubated statically at 30 °C for 7–9 days.

2.3. Purification of BC membrane

After incubation, bacterial cellulose membrane produced on the surface of the liquid culture medium was harvested and purified by boiling them in 1.0% NaOH solution for 2 h, and subsequently in distilled water for another 2 h. The two steps were repeated for three cycles to remove medium components and attached cells. After that, the BC membrane was thoroughly washed with distilled water until the pH of the washing liquid was neutral and finally immersed in the distilled water prior to use.

2.4. In situ preparation of AgNPs impregnated BC composites

The BC/AgNPs composite was prepared as follows: the BC membrane was immersed in 10 ml of 1 mM $AgNO_3$ solution at 30 °C for 0.5 h protected from light, and then picked up and rinsed in 20 ml of 5 mM $NaBH_4$ solution at 0 °C for another 0.5 h. Subsequently, the membrane was washed with 3 ml × 10 ml of ultra-pure water to remove the excess chemicals and freeze-dried (LYQQLEST-55, Telstar, Spain) for 24 h before use.

2.5. Characterization

For SEM analysis, samples cut from the freeze-dried bacterial cellulose membranes were coated with a thin layer of evaporated gold, and the images were taken using a JEOL, JSM-5600LV scanning electron microscope (Japan) with an acceleration voltage of 15 kV. Transmission electron microscopy (TEM) images were recorded using a HITACHI, H-800 transmission electron microscope (Japan) operating at an acceleration voltage of 15 kV. For TEM measurements, samples were prepared by dropping 10–20 μl of finely ground BC/AgNPs composite dispersions on a copper grid and dried at room temperature after removing excess solution using filter paper. The particle sizes of the AgNPs were measured using Image J software. At least 100 particles of each sample from different TEM images were analyzed. The histogram of the size distribution was established by Origin software. Nitrogen physisorption measurements were performed by a JW-BK Brunauer–Emmett–Teller (BET) surface area analyzer (Beijing JWGB Sci. & Tech. Co., Ltd., China). Before determination, the accurately weighted freeze-dried samples were put in sample tubes and heated at 90 °C in vacuum for 1.5 h to remove surface moisture and other contaminants. The BET analysis was done for relative vapor pressure of 0.05–0.25. X-ray diffraction spectra were recorded using a D/Max-2550PC diffractometer (Japan) at 40 kV and 200 mA. Angular scanning was continued 5–60° (2θ) at 1°/min. The crystallite index (CrI^{XRD}) was calculated using empirical method for native cellulose: $CrI^{XRD} = (I_{200} - I_{am})/I_{200} \times 100\%$, where I_{200} was the maximum intensity of the (2 0 0) lattice diffraction and I_{am} was the intensity diffraction at $2\theta = 18°$ (Segal, Creely, Martin, & Conrad, 1959). The content of silver in the composite was quantified by inductively coupled plasma (ICP) equipment (Prodigy, LEEMAN, USA) with the sample dissolved in 95% nitric acid. Elemental maps of the composite were obtained using energy dispersive X-ray spectrometer (EDX, IE 300X, Oxford; JSM-5600LV scanning electronic microscope). The optical absorption of the BC/AgNPs composite was measured using a UV-1100 spectrometer (Shanghai Techcomp Instrument Ltd., China). Triplicate experiments for each sample were carried out.

2.6. Assay of antimicrobial activity

The antimicrobial activity of the BC/AgNPs composite was investigated against *E. coli* as the model Gram-negative bacteria and *S. aureus* as the model Gram-positive bacteria, which were precultured at 37 °C to reach a concentration of about 10^8 colony forming unit/ml (CFU/ml). All the test samples were cut into circular discs (15 mm in diameter, 1.2–1.3 mg in weight) for use. Two methods, i.e. the zone of inhibition and log reduction test were adopted to evaluate the antimicrobial activity. For the zone of inhibition method, the control and the test samples were placed on the *E. coli* or *S. aureus* growth agar plate and incubated at 37 °C for 24 h. The inhibition zone was calculated by measuring the diameter of

the nearest whole millimeter of the inhibited growth around the sample disk, and was performed in triplicates. The log reduction test was performed to quantitatively evaluate the antimicrobial activity. In this case, 0.1 ml of the test bacterial suspensions were transferred onto the sample, and then incubated under sterile condition at room temperature for 18 h. After that, the sample was treated by 50 ml, 0.03 M of PBS buffer to wash off the bacteria grown on it. Different dilutions of the bacterial suspensions were then transferred onto nutrient agar plates, and the viable bacteria were monitored by counting the number of colony-forming units from the appropriate dilution on nutrient agar plates and expressed as CFU. The same procedure was performed on pure BC membrane without Ag addition as control. The antimicrobial effect of the composite sample was evaluated by three forms, i.e. bactericidal activity, bacteriostatic activity and reduction ratio, and calculated using the following equations (Pinto et al., 2009): Bactericidal activity = Log CFU T_0 control − Log CFU T_{18} composite; Bacteriostatic activity = Log CFU T_{18} control − Log CFU T_{18} composite; Killing ratio = (CFU T_{18} control − CFU T_{18} composite)/CFU T_{18} control × 100%, where CFU T_0 control and CFU T_{18} control meant the viable bacterial number for the control sample at 0 h and 18 h contact time, respectively, while CFU T_{18} composite represented the bacterial survival number for the BC/AgNPs composite sample at 18 h contact time.

3. Results and discussion

3.1. Preparation and characterization of BC membrane from different fermentation carbon sources

In this study, the production of bacterial cellulose membranes was performed by static culture using different fermentation medium especially carbon sources, i.e. glucose, maltose and sucrose. It was found that a white, near transparent gel sheet of bacterial cellulose generated at the surface of the culture medium of every test carbon source. The SEM analysis was applied to observe the micromorphology of the BC membranes. It was turned out that the BC materials prepared by every test carbon source exhibited a similar nanoporous three-dimensional network structure with the ribbons of nanofibrils 60–100 nm wide from the surface morphology of the sample (Fig. 1). Moreover, the porous properties and crystallinity of the BC materials from various carbon sources were analyzed by nitrogen physisorption measurements and XRD method (Fig. 2), respectively. As listed in Table 1, the glucose- and maltose-derived BC membranes possessed similar structure characteristics in porosity and crystallinity, while the sucrose-derived sample was much smaller in both the two aspects.

3.2. In situ preparation of silver nanoparticles on BC membrane

It was reported that the structure of the three-dimensional networks and large amount of the nanosized pores in the BC materials acted as the nanoreactors for the nucleation and growth of the silver particles during in situ synthesis by the template method (Maneerung et al., 2008). In this work, various BC membranes produced by different carbon sources were utilized as the template to in situ prepare silver nanoparticles. Fig. 3a and b showed the photographs of the BC membrane before and after silver impregnation. As seen in the pictures, the reaction could be easily monitored from the color evolution of the membrane. Visual observation showed that as the reaction proceeded, the color shifted from white to bright yellow, thus signifying the formation of the silver nanoparticles in the membrane. (For interpretation of the references to color in this sentence, the reader is referred to the web version of the article.) This conclusion was further confirmed by the energy dispersive X-ray (EDX) and UV–vis analysis, respectively. Similar EDX spectra of the silver-impregnated BC composite from the three test carbon sources were obtained and the evidences of the elemental silver were presented (see Fig. 4a). Fig. 4b showed the UV–vis absorption spectra of the composite sample. An absorption band with a peak at 409 nm appeared, which was assigned to silver nanoparticles due to the surface plasmon resonane (SPR) (Dubas & Kumlangdudsana, 2006; Mingwei, Guodong, Guanjun, Zhiyu, & Minquan, 2006; Vimala, Sivudu, Mohan, Sreedhar, & Raju, 2009). This peak at 409 nm confirmed that the size of the silver nanoparticles was approximately between 4 and 20 nm, which was reported in other literatures (Cai et al., 2009; Khalil-Abad, Yazdanshenas, & Nateghi, 2009).

The size and size distribution of the AgNPs formed on the different BC membranes were analyzed by means of transmission electron microscopy (TEM) (Fig. 5), and the histogram based on the TEM images illustrated their average size and size distribution. As seen in the figures, the AgNPs formed in every test BC membrane exhibited a small size and a narrow size distribution. The data on particle size distribution revealed the presence of AgNPs in the size range of 5–14 nm, with an average size 8.3, 9.8 and 7.9 nm for the maltose, glucose and sucrose-derived sample, respectively. This result was in very good agreement with that obtained by UV–vis

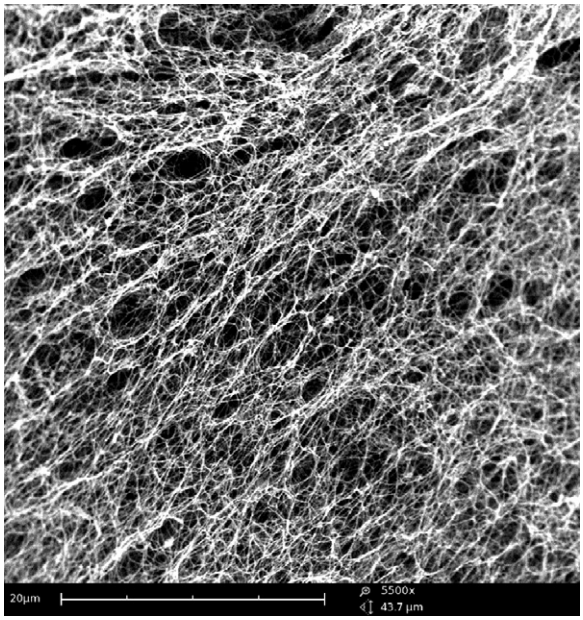

Fig. 1. SEM image of the BC membrane obtained from maltose.

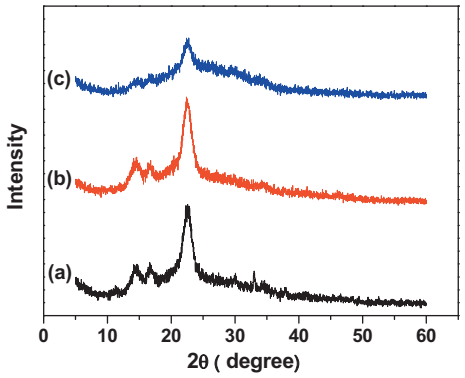

Fig. 2. X-ray diffraction patterns of BC membranes from glucose (a), maltose (b) and sucrose (c) as the carbon source.

Table 1
The structure properties of the BC membranes from different carbon sources.

Carbon source	Surface area (m^2/g)	Pore volume (cm^3/g)	Average pore size (nm)	Crystallinity^{XRD} (%)
Glucose	86.94	0.25	11.45	76.91
Maltose	82.60	0.23	10.97	78.44
Sucrose	60.89	0.17	11.11	69.10

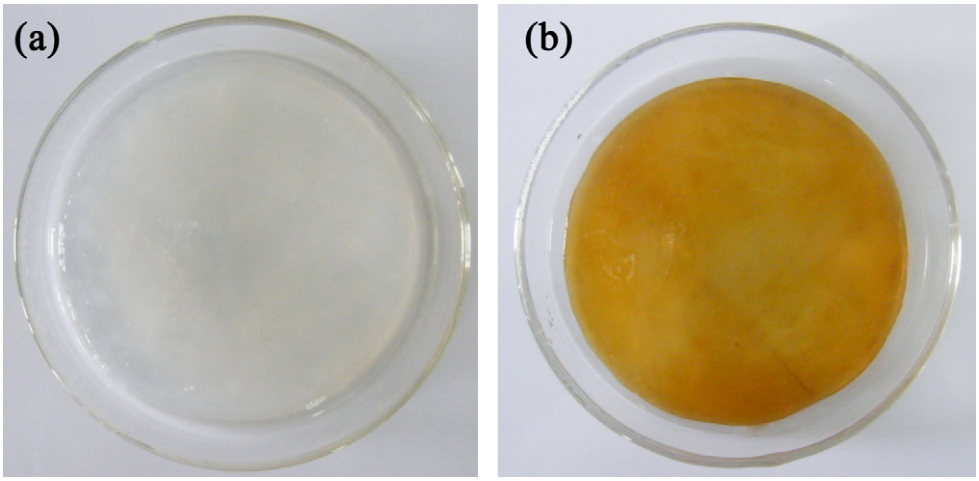

Fig. 3. Photographs of a pure BC membrane (a) and a BC/AgNPs composite (b).

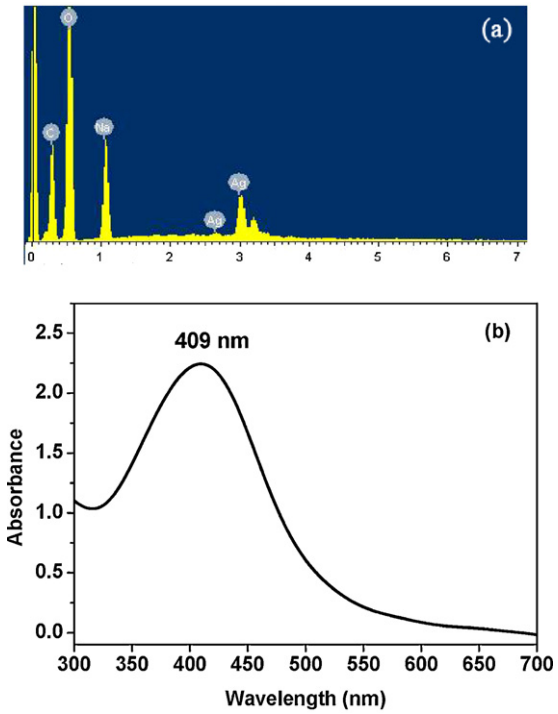

Fig. 4. EDX spectra (a) and UV–vis spectra (b) of a BC/AgNPs composite obtained from maltose.

spectroscopy in our work, as well as those reported in other literatures about the size and size distribution of AgNPs analyzed by TEM (Cai et al., 2009; Maneerung et al., 2008). Therefore, it was proved again that the BC matrix served as a stabilizing template for the formation of silver nanoparticles and prevented them from further aggregation. The literatures (Cai et al., 2009; Maneerung et al., 2008) reported that when bacterial cellulose was immersed in the aqueous $AgNO_3$, silver ions were readily penetrated into bacterial cellulose through the porous structure and bound to its microfibrils probably via electrostatic interactions, because the electron-rich oxygen atoms of polar hydroxyl and ether groups of bacterial cellulose were expected as active sites to interact with electropositive transition metal cations. After reduction in aqueous $NaBH_4$, silver ions were reduced to form silver nanoparticles. Since the structure of bacterial cellulose was three-dimensional networks and comprised large amount of pores (see Fig. 1), the nanosized pores just acted as the nanoreactors for the nucleation and growth of the silver particles, and could also restrict the growth of particles within the pores and lock up the content of silver nanoparticles.

The silver contents of the BC/AgNPs composites from different carbon sources were determined by elemental analysis using ICP, and the results were illustrated in Fig. 6. The mass contents of silver in the composites ranged from 0.86 to 1.60% depending upon the used carbon source. By associating the silver content with the crystallinity of the BC membrane, it was found that the sucrose-derived BC membrane, which possessed the lowest crystallinity, exhibited the highest silver content. This might demonstrate that the Ag^+ adsorption was favored mainly by the amorphous phase of BC microfibrils. The decrease in the density of the amorphous phase could retard the Ag^+ adsorption action within the highly crystalline BC membrane, thus resulting in a low silver content after $NaBH_4$ reduction.

3.3. Antimicrobial activity of BC/AgNPs composite membrane

Infection is a significant cause of delayed or prolonged wound healing, and high bacterial levels interferes with the progression of wound healing. Silver has long been known to have strong bactericidal effects as well as a broad spectrum of antimicrobial activities. However, the mechanism of the bactericidal effect of silver (Ag^+ or Ag^0) is presently still unclear. Several studies proposed that silver nanoparticles acted primarily in three ways: (1) nanoparticles might attach to the surface of the bacterial cell membrane disturbing permeability and respiration functions of the cell; (2) they could penetrate inside the bacteria and cause further damage by possibly interacting with sulfur- and phosphorus-containing compounds such as DNA; (3) nanoparticles might release silver ions as

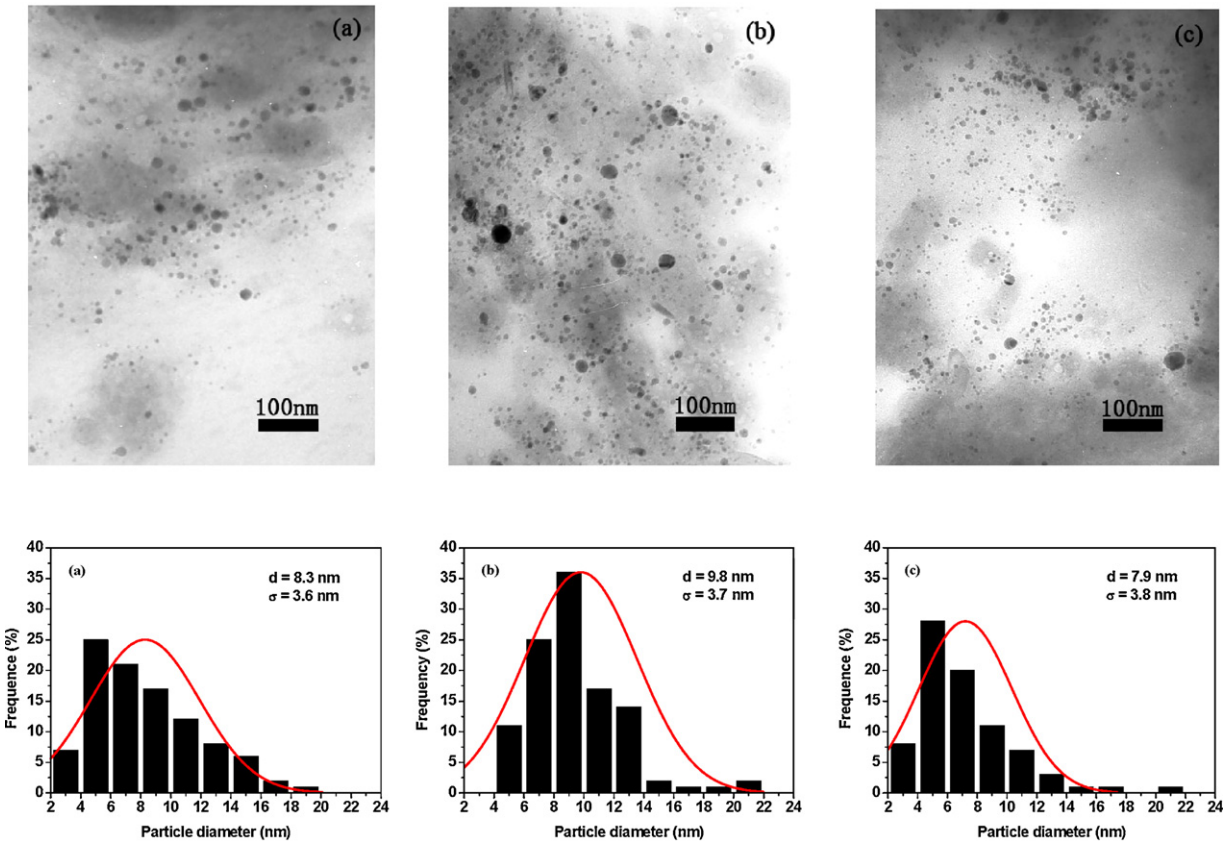

Fig. 5. TEM images and particle size distribution histograms of silver nanoparticles formed in BC membranes prepared from maltose (a), glucose (b) and sucrose (c) as the carbon source.

Fig. 6. The silver contents of the BC/AgNPs composites from different carbon sources.

an additional contribution to the bactericidal effect. Smaller size of AgNPs with larger surface area available for interaction would give stronger bactericidal effect than the larger size particles (Morones et al., 2005; Kvítek et al., 2008). In this study, the antimicrobial activities of the BC/AgNPs composites prepared from different carbon sources were tested against *E. coli* and *S. aureus* by the zone of inhibition and log reduction methods, respectively.

Regarding the assay by zone of inhibition, every test BC/AgNPs composite exhibited an obvious inhibition zone against both the two model bacteria, while no inhibition zone was observed for the pure bacterial cellulose. This demonstrated that the antimicrobial activity existed only due to silver nanoparticles impregnated inside bacterial cellulose and not due to bacterial cellulose itself. Moreover, all the test composite samples produced a wider inhibition zone against *S. aureus* than *E. coli*. Taking the BC/AgNPs composite and pure BC membrane obtained from maltose for an example, the widths of the inhibition zones of the composite were about 2 mm for *E. coli*. and 9 mm for *S. aureus*, respectively, and no inhibition zone was found for the pure BC membrane, as displayed in Fig. 7.

The quantitative assay of antimicrobial activity of the BC/AgNPs composites derived from different carbon sources was conducted and three parameters were calculated for comparison (see in Table 2). Generally, low antimicrobial activity was considered to be less than a 1-log reduction, moderate activity between a 1- and 3-log reduction, and high antimicrobial activity was greater than a 3-log reduction (Gallant-Behm et al., 2005). As seen from the data, all the test BC/AgNPs composites exhibited a moderate or high antimicrobial effect against both the two model bacteria with the log reduction above 1. However, the most notable antibacterial effect was observed not for the composite with the highest silver content in the sucrose-derived composite, but for the sample with a relative high silver content, i.e. maltose-derived composite. The possible reasons behind the phenomena were mainly attributed to the microstructure of the BC template, i.e. pore volume and surface area. The BC membrane with higher pore volume and surface area might encourage Ag^+ or AgNPs to pass through the membrane and release into the outer environment, thus realizing a stronger antimicrobial effect. Among all the test BC/AgNPs composites, the sample derived from maltose with a silver content of 1.06% realized a more than 8-log reduction and >99.99% killing ratio in the number of viable *E. coli* (no viable bacteria colony was found by three dilutions on nutrient agar plates) after contact for 18 h. That is to say, 1.2 mg of the BC/AgNPs composite was sufficient to ensure no detectable growth of *E. coli* in 0.1 ml of medium with a bacteria concentration of about 10^8 CFU/ml.

Moreover, it was found that there was no consistency in the antimicrobial activity of the BC/AgNPs composites determined by

Table 2
Comparison of quantitative antimicrobial activity assay of BC/AgNPs composites from different carbon sources tested against *E. coli* and *S. aureus.*

Carbon sources	*E. coli* (Gram$^-$)			*S. aureus* (Gram$^+$)		
	Bactericidal activity (log reduction)	Bacteriostatic activity (log reduction)	Killing ratio (%)	Bactericidal activity (log reduction)	Bacteriostatic activity (log reduction)	Killing ratio (%)
Glucose	3.30	2.55	99.72	1.32	1.06	91.18
Maltose	8.93	8.19	> 99.99	2.01	1.74	98.16
Sucrose	3.54	2.80	99.84	1.97	1.70	97.99

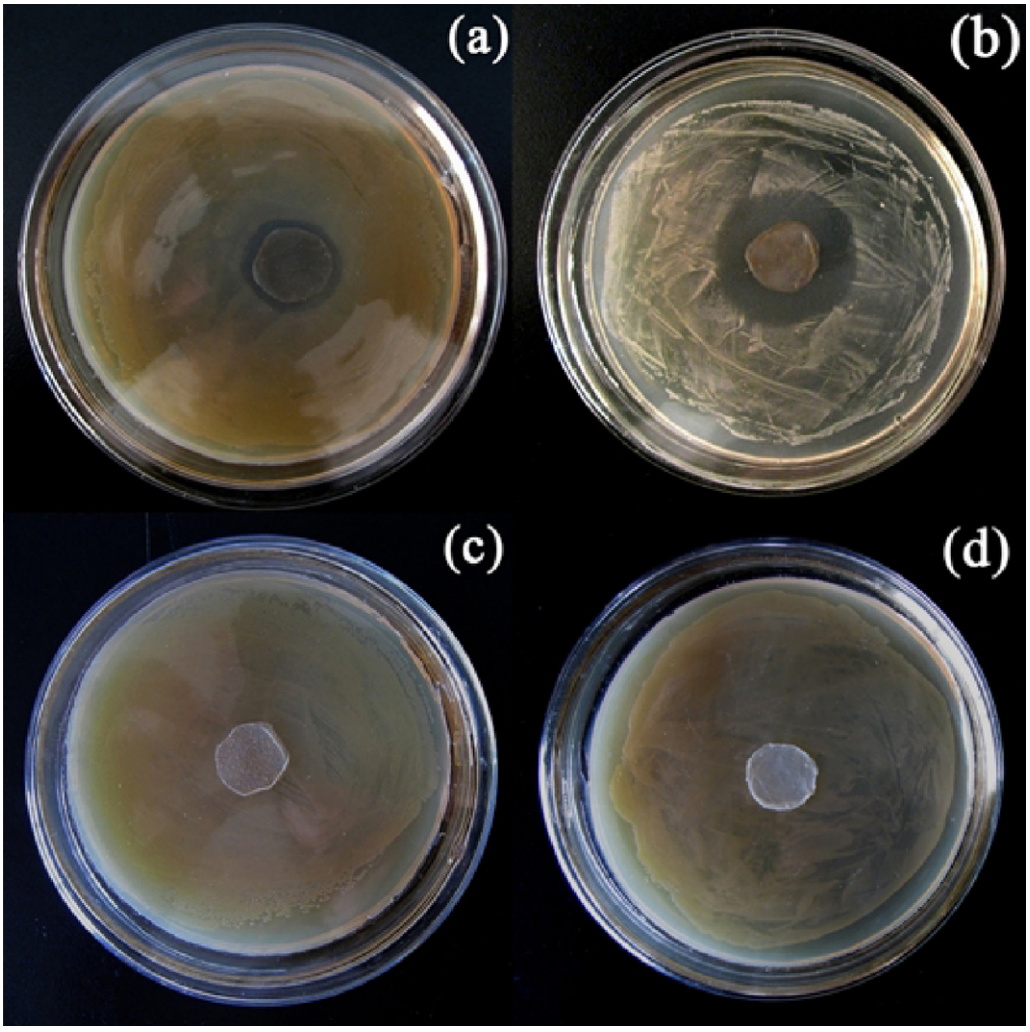

Fig. 7. Photograph images of the inhibition zone of BC/AgNPs composite against *Escherichia coli* (a) and *Staphylococcus aureus* (b), and pure BC against *Escherichia coli* (c) and *Staphylococcus aureus* (d).

the two test methods used herein, that is, superior susceptibility of the composite was achieved to *S. aureus* (Gram$^+$) by zone of inhibition method, while *E. coli* (Gram$^-$) by log reduction assay. Similar results have been reported previously. Gallant-Behm et al. (2005) compared the two in vitro test methods, i.e. zone of inhibition and log reduction assays, by determining the antimicrobial activities of seven commercial silver-containing dressings against 17 clinically relevant microorganisms. It was turned out that the two methods did not generate similar results and not correlate at all. The authors proposed that this was most likely due to the reactivity of silver ions with Cl^- and other inorganic moieties such as sulfide and organic molecules (e.g. proteins and peptides in serum) in the medium of the zone of inhibition test, limiting the diffusion of silver and thus invalidating the test results. This report concluded that zone of inhibition data generated for silver-containing dressings was of little value and that log reduction assay was of greater use for evaluating the antimicrobial efficacy of silver-containing dressings.

4. Conclusions

In this study, silver nanoparticles were in situ synthesized in the bacterial cellulose membranes by template method, and the influences of the micro-structure of the template matrix, i.e. the BC membrane produced by different fermentation carbon sources, were investigated on the formation of the silver nanoparticles. The results indicated that the structure of the three-dimensional networks and large amount of the nanosized pores in the BC materials served as a stabilizing template for the formation of silver nanoparticles, with the presence of AgNPs in the size range of 5–14 nm and a similar average particle size (<10 nm) for every test BC membrane

template. The mass contents of silver in the composites ranged from 0.86 to 1.60% depending upon the used carbon source, and the sucrose-derived BC membrane, which possessed the lowest crystallinity, exhibited the highest silver content. The antimicrobial activity of every test BC/AgNPs composite was evaluated by both zone of inhibition and log reduction methods, and strong bactericidal effects were observed by every composite sample towards both *E. coli* and *S. aureus* bacteria. Among them, the sample derived from maltose with a silver content of 1.06% realized a more than 8-log reduction and >99.99% killing ratio in the number of viable *E. coli* after contact for 18 h. That is to say, 1.2 mg of the silver contained composite was sufficient to ensure no detectable growth of *E. coli* in 0.1 ml of medium with a bacteria concentration of about 10^8 CFU/ml.

Acknowledgments

The project was funded by the Chinese National Natural Science Foundation (No. 21004008), the Shanghai Municipal Education Commission and Shanghai Education Development Foundation ("Chen Guang" project, No. 11CG35), the Science and Technology Commission of Shanghai Municipality (0852nm03500), and the Fundamental Research Funds for the Central Universities. All the financial support is gratefully acknowledged.

References

Barud, H. S., Barrios, C., Regiani, T., Marques, R. F. C., Verelst, M., Dexpert-Ghys, J., et al. (2008). Self-supported silver nanoparticles containing bacterial cellulose membranes. *Materials Science and Engineering C*, *28*, 515–518.

Bhattacharjee, R. R., & Mandal, T. K. (2007). Polymer-mediated chain-like self-assembly of functionalized gold nanoparticles. *Journal of Colloid and Interface Science*, *307*, 288–295.

Cai, J., Kimura, S., Wada, M., & Kuga, S. (2009). Nanoporous cellulose as metal nanoparticles support. *Biomacromolecules*, *10*, 87–94.

Clasen, C., Wilhelms, T., & Kulicke, W. M. (2006). Formation and characterization of chitosan membranes. *Biomacromolecules*, *7*, 3210–3222.

Cui, Y. M., Liu, L., Li, B., Zhou, X. F., & Xu, N. P. (2010). Fabrication of tunable core–shell structured TiO_2 mesoporous microspheres using linear polymer polyethylene glycol as templates. *The Journal of Physical Chemistry C*, *114*, 2434–2439.

Czaja, W., Krystynowicz, A., Bielecki, S., & Brown, R. M. (2006). Microbial cellulose – The natural power to heal wounds. *Biomaterials*, *27*, 145–151.

Czaja, W. K., Young, D. J., Kawecki, M., & Brown, R. M. (2007). The future prospects of microbial cellulose in biomedical applications. *Biomacromolecules*, *8*, 1–12.

Dubas, S. T., & Kumlangdudsana, P. P. (2006). Layer-by-layer deposition of antimicrobial silver nanoparticles on textile fibers. *Colloids and Surfaces A: Physicochemical and Engineering Aspects*, *289*, 105–109.

Gallant-Behm, C. L., Yin, H. Q., Liu, S., Heggers, J. P., Langford, R. E., Olson, M. E., et al. (2005). Comparison of in vitro disc diffusion and time kill-kinetic assays for the evaluation of antimicrobial wound dressing efficacy. *Wound Repair and Regeneration*, *13*, 412–421.

Hu, W. L., Chen, S. Y., Li, X., Shi, S. K., Shen, W., Zhang, X., et al. (2009). In situ synthesis of silver chloride nanoparticles into bacterial cellulose membranes. *Materials Science and Engineering C*, *29*, 1216–1219.

Jonas, R., & Farah, L. H. (1998). Production and application of microbial cellulose. *Polymer Degradation and Stability*, *59*, 101–106.

Khalil-Abad, M. S., Yazdanshenas, M. E., & Nateghi, M. R. (2009). Effect of cationization on adsorption of silver nanoparticles on cotton surfaces and its antibacterial activity. *Cellulose*, *16*, 1147–1157.

Klasen, H. J. (2000a). Historical review of the use of silver in the treatment of burns. I. Early uses. *Burns*, *26*, 117–130.

Klasen, H. J. (2000b). Historical review of the use of silver in the treatment of burns. I. Early uses. *Burns*, *26*, 131–138.

Kvítek, L., Panáček, A., Soukupová, J., Kolář, M., Večeřová, R., Prucek, R., Holecová, M., & Zbořil, R. (2008). Effect of surfactants and polymers on stability and antibacterial activity of silver nanoparticles (NPs). *The Journal of Physical Chemistry C*, *112*, 5825–5834.

Lansdown, A. B. G. (2002). Silver I: Its antibacterial properties and mechanism of action. *Journal of Wound Care*, *11*, 125–130.

Leaper, D. J. (2006). Silver dressings: Their role in wound management. *International Wound Journal*, *3*, 282–294.

Lee, S. W., Mao, C., Flynn, C. E., & Belcher, A. M. (2002). Ordering of quantum dots using genetically engineered viruses. *Science*, *296*, 892–895.

Li, X., Chen, S. Y., Hu, W. L., Shi, S. K., Shen, W., Zhang, X., & Wang, H. P. (2009). In situ synthesis of CdS nanoparticles on bacterial cellulose nanofibers. *Carbohydrate Polymers*, *76*, 509–512.

Maneerung, T., Tokura, S., & Rujiravanit, R. (2008). Impregnation of silver nanoparticles into bacterial cellulose for antimicrobial wound dressing. *Carbohydrate Polymers*, *72*, 43–51.

Mingwei, Z., Guodong, Q., Guanjun, D., Zhiyu, W., & Minquan, W. (2006). Plasma resonance of silver nanoparticles deposited on the surface of submicron silica spheres. *Materials Chemistry and Physics*, *96*, 489–493.

Morones, J. R., Elechiguerra, J. L., Camacho, A., Holt, K., Kouri, J., Ramírez, J. T., et al. (2005). The bactericidal effect of silver nanoparticles. *Nanotechnology*, *16*, 2346–2353.

Nyamjav, D., & Ivanisevic, A. (2005). Templates for DNA-templated Fe_3O_4 nanoparticles. *Biomaterials*, *26*, 2749–2757.

Pinto, R. J. B., Marques, P. A. A. P., Neto, C. P., Trindade, T., Daina, S., & Sadocco, P. (2009). Antibacterial activity of nanocomposites of silver and bacterial or vegetable cellulosic fibers. *Acta Biomaterialia*, *5*, 2279–2289.

Rai, M., Yadav, A., & Gade, A. (2009). Silver nanoparticles as a new generation of antimicrobials. *Biotechnology Advances*, *27*, 76–83.

Robson, M. C. (1997). Wound infection: A failure of wound healing caused by an imbalance of bacteria. *Surgical Clinics of North America*, *77*, 637–650.

Segal, L., Creely, J. J., Martin, A. E. J., & Conrad, C. M. (1959). An empirical method for estimating the degree of crystallinity of native cellulose using the X-ray diffractometer. *Textile Research Journal*, *29*, 786–794.

Uppal, R., Ramaswamy, G. N., Arnold, C., Goodband, R., & Wang, Y. (2011). Hyaluronic acid nanofiber wound dressing – Production characterization, and in vivo behavior. *Journal of Biomedical Materials Research Part B Applied Biomaterials*, *97B*, 20–29.

Vimala, K., Sivudu, K. S., Mohan, Y. M., Sreedhar, B., & Raju, K. M. (2009). Controlled silver nanoparticles synthesis in semi-hydrogel networks of poly(acrylamide) and carbohydrates: A rational methodology for antibacterial application. *Carbohydrate Polymers*, *75*, 463–471.

Wei, B., Yang, G., & Hong, F. (2011). Preparation and evaluation of a kind of bacterial cellulose dry films with antibacterial properties. *Carbohydrate Polymers*, *84*, 533–538.

Wiegand, C., Heinze, T., & Hipler, U. (2009). Comparative in vitro study on cytotoxicity, antimicrobial activity, and binding capacity for pathophysiological factors in chronic wounds of alginate and silver-containing alginate. *Wound Repair and Regeneration*, *17*, 511–521.

Wu, M., Kuga, S., & Huang, Y. (2008). Quasi-one-dimensional arrangement of silver nanoparticles templated by cellulose microfibrils. *Langmuir*, *24*, 10494–10497.